

The (${}^8\text{Li}, \alpha$) reaction at low energy: Direct ${}^4\text{H}$ cluster transfer?

F. D. Becchetti,¹ R. S. Raymond,¹ D. A. Roberts,¹ J. Lucido,¹ P. A. DeYoung,² B. Hilldore,² J. Bychowski,^{2,3} A. J. Huisman,² P. J. VanWylen,² J. J. Kolata,³ G. Rogachev,⁴ and J. D. Hinnefeld⁵

¹*Department of Physics, University of Michigan, Ann Arbor, Michigan 48109-1120, USA*

²*Department of Physics and Engineering, Hope College, Holland, Michigan 49422-9000, USA*

³*Department of Physics, University of Notre Dame, Notre Dame, Indiana 46556-5670, USA*

⁴*Department of Physics, Florida State University, Tallahassee, Florida 32306-4350, USA*

⁵*Department of Physics, Indiana University—So. Bend, South Bend, Indiana 46634-7111, USA*

(Received 17 May 2004; revised manuscript received 9 February 2005; published 31 May 2005)

The (${}^8\text{Li}, \alpha$) reaction has been studied at $E({}^8\text{Li}) = 27.7$ MeV on targets of ${}^{\text{nat}}\text{C}$, ${}^{27}\text{Al}$, and ${}^{208}\text{Pb}$ using a secondary ${}^8\text{Li}$ beam. The α -energy spectra for ${}^{27}\text{Al}$ and ${}^{208}\text{Pb}$ are generally nondistinct and resemble fragmentation spectra. In contrast, data for the ${}^{\text{nat}}\text{C}$ target exhibit enhanced (${}^8\text{Li}, \alpha$) cross sections in the region corresponding to population of low-lying levels in ${}^{16}\text{N}$. Angular distributions were determined over a large angular range and exhibit a strong forward peaking for ${}^{27}\text{Al}$ and some forward peaking for the ${}^{\text{nat}}\text{C}$ data. They are otherwise rather featureless but distinct from spectra expected from fusion evaporation. The data for ${}^{27}\text{Al}$ are indicative of either direct or sequential fragmentation processes. Similar analysis of limited data obtained at $E({}^8\text{Li}) = 27.7$ MeV for the ${}^{208}\text{Pb}$ target, along with data previously obtained at higher ${}^8\text{Li}$ energies, is suggestive of a sequential breakup mechanism. In the case of the ${}^{\text{nat}}\text{C}$ target, the data corresponding to low excitation energies in ${}^{16}\text{N}$ exhibit (${}^8\text{Li}, \alpha$) angular distributions that appear to be most consistent with a ${}^4\text{H}$ transfer mechanism. However, we cannot distinguish between a one-step ${}^4\text{H}$ cluster transfer and a multistep ${}^4\text{H}$ transfer (such as $n + {}^3\text{H}$).

DOI: 10.1103/PhysRevC.71.054610

PACS number(s): 25.60.Je, 25.60.Gc, 27.20.+n

I. INTRODUCTION

A first-generation study of ${}^8\text{Li}$ -induced reactions on various targets at $E({}^8\text{Li}) = 14.8$ MeV using the University of Michigan (UM)—University of Notre Dame (UND) 3.5T “*LilSol*” solenoid radioactive nuclear beam (RNB) apparatus [1–3] at UND revealed some interesting features [4,5] for ${}^8\text{Li}$ -induced reactions on ${}^{\text{nat}}\text{C}$. In particular, the spectra and angular distributions [4] for the highly exothermic ${}^{12}\text{C}({}^8\text{Li}, \alpha){}^{16}\text{N}$ reaction ($Q = +12.8$ MeV) exhibited features suggestive of a direct multinucleon transfer mechanism. This included evidence (although with very limited data) for selective population of states (or multiplets) in ${}^{16}\text{N}$ and as well as what could be interpreted as a diffractionlike angular distribution for these levels. It was suggested that direct ${}^4\text{H}$ cluster transfer might be responsible [6], but counterarguments were also given [7]. In order to further elucidate the (${}^8\text{Li}, \alpha$) reaction mechanism, we have performed a followup experiment at a higher ${}^8\text{Li}$ energy ($E = 27.7$ MeV), and in addition to ${}^{\text{nat}}\text{C}$, have measured ${}^{27}\text{Al}$ (${}^8\text{Li}, \alpha$) and ${}^{208}\text{Pb}$ (${}^8\text{Li}, \alpha$) energy spectra and angular distributions at both forward and backward angles. These data are then compared with calculations for various reaction models.

II. EXPERIMENT

The experiment was performed at the UND nuclear structure laboratory using the UM–UND “*TwinSol*” double-solenoid RNB system [8,9]. A 27.7 MeV secondary ${}^8\text{Li}$ beam of 10^5 to 10^6 /s was produced from a 31.4 MeV primary ${}^7\text{Li}$ beam incident on a gas-cooled ${}^9\text{Be}$ production target. The secondary-beam reaction targets consisted of natural carbon (98.9% ${}^{12}\text{C}$) of areal density, $\rho x = 0.93$ mg/cm²;

natural aluminum (100% ${}^{27}\text{Al}$), $\rho x = 1.3$ mg/cm²; and >99% enriched ${}^{208}\text{Pb}$, $\rho x = 1.8$ mg/cm². The magnet system was operated in the “crossover” mode with a thin energy-loss absorber and collimator placed between the magnets to help reduce interference from other secondary-beam products, in particular ${}^4\text{He}^{++}$. Likewise, the intense scattered ${}^7\text{Li}$ ions from the primary beam were stopped in a stop set at the ${}^7\text{Li}$ focal point after the first magnet. The primary beam was monitored in a faraday cup located behind the production target.

Given the very positive Q values for the two-body direct (${}^8\text{Li}, \alpha$) transfer reactions of interest, the ${}^4\text{He}$ beam contaminant was generally well separated in energy from most of the α -particle reaction products. Nonetheless, this contaminant limited measurements of the α spectra to energies above the ${}^4\text{He}$ beam energy, especially for the ${}^{208}\text{Pb}$ target ($Q = 4.9$ MeV; see Fig. 1). In later, related *TwinSol* experiments [10], time of flight was utilized to separate the ${}^4\text{He}$ contaminant in the secondary beam from α particles produced in ${}^8\text{Li}$ -induced reactions.

The α -particle reaction products were detected with a set of ΔE - E Si telescopes located in an ~ 50 cm diameter scattering chamber situated after the second magnet [8,9]. The reaction-product detectors consisted of 290 to 420 μm ΔE Si surface-barrier detectors backed by similar 400 to 1100 μm E detectors to form an array of five ΔE - E telescopes with combined thickness sufficient to stop the most energetic α particles expected (~ 50 MeV; see Fig. 1). The detectors were mounted on two moveable tables in the scattering chamber to provide angle measurements from 15 to 150° (lab). In addition, a position-sensitive ΔE - E Si detector system was used both to determine the focus [8] of the secondary ${}^8\text{Li}$ beam ($\theta = 0^\circ$)

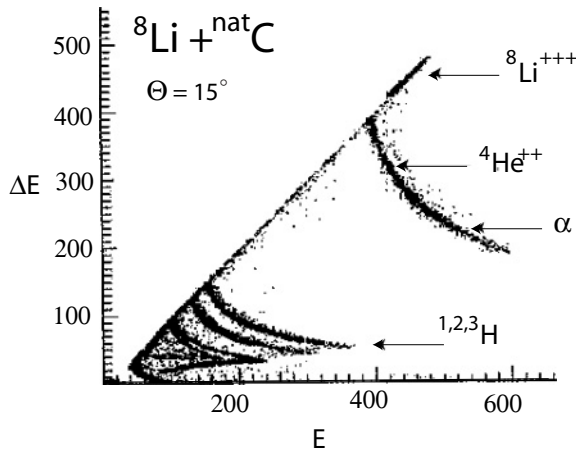


FIG. 1. A sample E - E Si detector telescope spectrum used for particle identification. The α -particle band from $({}^8\text{Li}, \alpha)$ is indicated together with the intense ${}^8\text{Li}^{+++}$ scattered beam and the α group arising from ${}^4\text{He}^{++}$ contamination of the secondary beam. The energy calibration is 60 keV/channel.

and to then serve as a ${}^8\text{Li}$ beam monitor (typically $\theta = 45^\circ$) via elastic scattering. The energy calibration of each detector telescope was determined using a ${}^{228}\text{Th}$ source ($E_\alpha = 8.78$ to 5.42 MeV).

The ${}^8\text{Li}$ beam spot at the secondary target location was about 5 mm in diameter full-width-at-half-maximum (FWHM) with a total angular spread of $\sim 6^\circ$. The detector telescopes were located approximately 14 cm from the target, and had

circular apertures which subtended 6° , yielding solid angles of 11 to 20 msr. Hence, the angular resolution was about 8° FWHM with an α energy resolution, mainly due to the secondary-beam energy spread and target energy loss, of typically 0.6 MeV FWHM. This would be sufficient to isolate certain groups of states. In particular, ${}^{27}\text{Al}$ was selected as a target since the residual ${}^{31}\text{Si}$ nucleus following a direct ${}^4\text{H}$ transfer has a number of low-lying states or groups of states [11] well separated in energy (e.g., $J^\pi = 1/2^+$, $E_x = 0.75$ MeV; $J^\pi = 5/2^+$, $E_x = 1.7$ MeV, etc.). Hence, these might be resolved if preferentially populated in the $({}^8\text{Li}, \alpha)$ reaction.

Selected α -particle spectra are shown in Figs. 2 and 3. Again, we note the highly exothermic nature of the direct $({}^8\text{Li}, \alpha)$ reaction with $Q = +12.8$ MeV, $Q = +24.3$ MeV, and $Q = +4.9$ MeV for ${}^{12}\text{C}$, ${}^{27}\text{Al}$, and ${}^{208}\text{Pb}$, respectively. In contrast, the Q value for breakup of ${}^8\text{Li}$ into $\alpha + (t + n)$ is $Q_{\text{bu}} = -4.5$ MeV.

As can be seen in Fig. 3, there is little evidence for selective population of low-lying (or other) levels in ${}^{31}\text{Si}$ from the ${}^{27}\text{Al}$ target. The α energies observed are far less than expected for a two-body direct ${}^4\text{H}$ transfer. This also seems to be true for the ${}^{208}\text{Pb}$ target (not shown), although owing to the low $E({}^8\text{Li})$, all reactions occur near or below the Coulomb barrier, and thus few if any high energy α s are observed at all (see below). Note that carbon and oxygen contaminants in the ${}^{208}\text{Pb}$ target also could contribute to the forward-angle data. In contrast, the α spectra (Fig. 2) for ${}^{\text{nat}}\text{C}({}^8\text{Li}, \alpha)$ exhibit α energies and enhanced cross sections corresponding to population of low-lying levels in ${}^{16}\text{N}$ [e.g., the four-state multiplet ($J^\pi = 2^-, 0^-$,

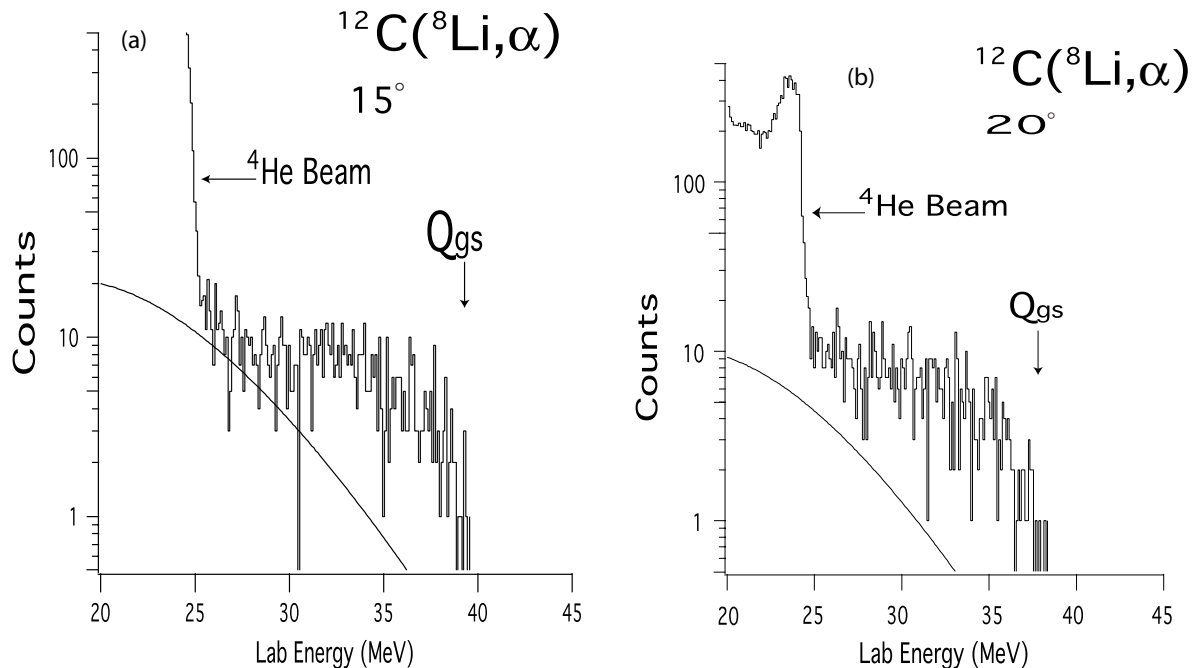


FIG. 2. Forward-angle α -particle energy spectra obtained for ${}^{\text{nat}}\text{C}$. The ground state (g.s.) Q value for a direct $({}^8\text{Li}, \alpha)$ reaction is indicated. The curves shown represent a fit (in the lab-frame) to the lower α -energy portion of the spectra using a one- or two-source moving-source fragmentation model with parameters noted in Figs. 4 and 5.

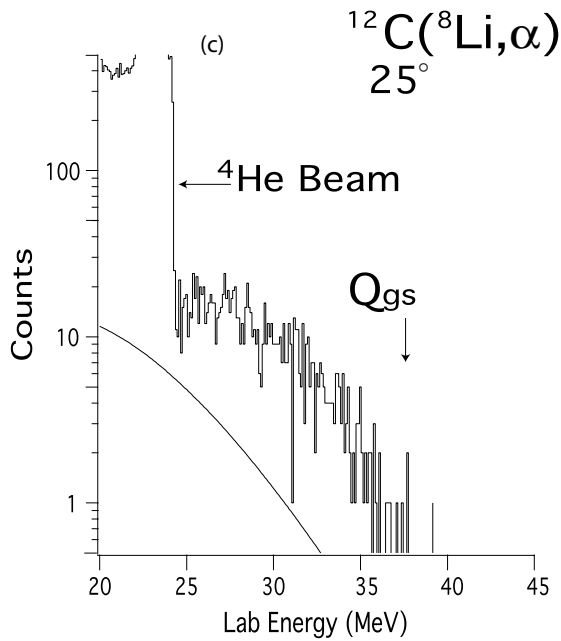


FIG. 2. (Continued.)

$3^-, 1^-$) near the $J^\pi = 2^-$ g.s.]. In particular, the spectra at the most forward angles [Fig. 2(a-c)] extend out to the high energy limit for a two-body transfer reaction ($Q = +12.8$ MeV, $E_{\alpha, \text{max}} \approx 40$ MeV). As noted above, a three-body breakup process ($Q = -4.5$ MeV) could not produce such high energy α particles.

Given the nature of most of the spectra, angular distributions were determined for various energy “bins.” These typically were 3 MeV wide in excitation energy and included the regions

cited above where known states exist. Some typical angular distributions are shown in Figs. 4 and 5. These are seen to be primarily forward peaked, with only modest α emission at large angles, i.e., beyond $\theta_{\text{lab}} = 90^\circ$. Thus, few if any events were observed at angles greater than 90° . This generally rules out simple fusion evaporation, i.e., α emission from a compound nucleus, as a major mechanism for producing α particles with $E_\alpha > 20$ MeV. Also, as suggested by the data, there is no distinct diffractionlike structure, at least relative to the experimental angular resolution ($\sim 8^\circ$ FWHM), for the ^{27}Al target (Fig. 5) and for much of the data for $^{\text{nat}}\text{C}$ (Fig. 4). Again, a possible exception appears to be the energy region [Fig. 4(a)] that would correspond to ($^8\text{Li}, \alpha$) resulting in low-excitation energy levels ($E_x \leq 9$ MeV) including the multiplet near the ground state in ^{16}N .

III. MODEL CALCULATIONS

We have done model calculations of the angular distributions for the following mechanisms: projectile breakup using moving-source or sequential breakup models [12–15], direct ^4H cluster transfer, and multistep nuclear transfer ($n + ^3\text{H}$).

A. Moving-source model

In the moving-source model [12–14], the Fermi motion of the α particle in the ^8Li projectile is calculated using an adjustable effective temperature T_α of typically a few MeV. At the time of breakup, the source of particle emission is described by a source velocity (v_R) relative to the incident projectile velocity (v_P), given as the ratio (v_R/v_P). The parameters T_α and (v_R/v_P) can be deduced by fitting the energy spectra and angular distributions of the breakup products, in this case the α particles. A value (v_R/v_P) = 1 indicates

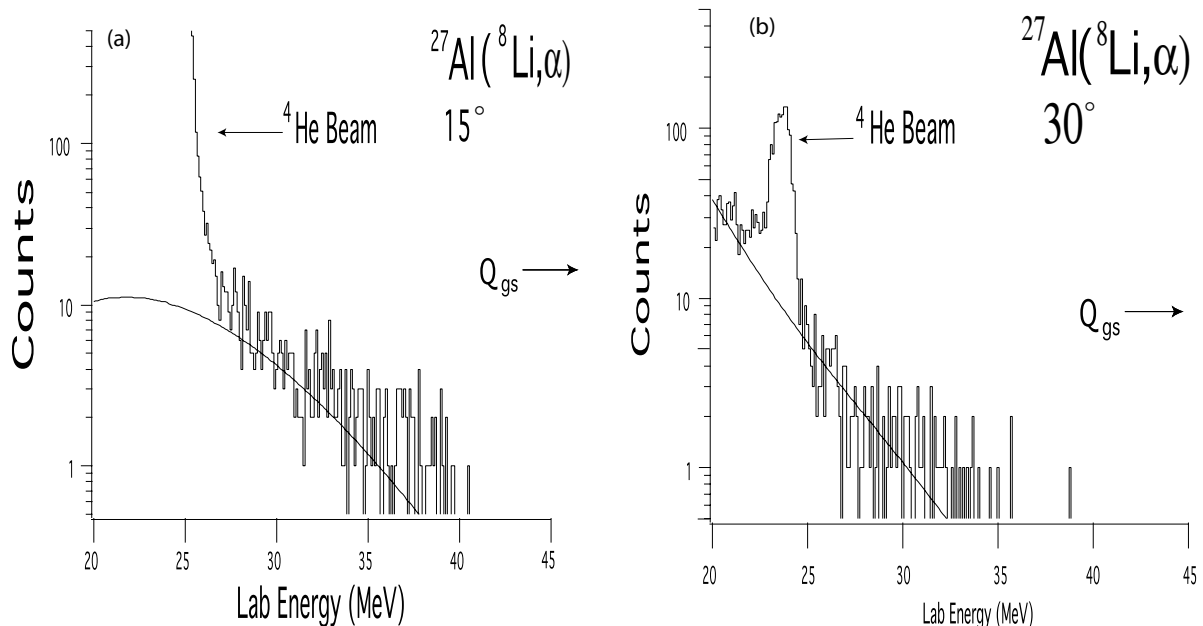


FIG. 3. Same as Fig. 2 but for an ^{27}Al target.

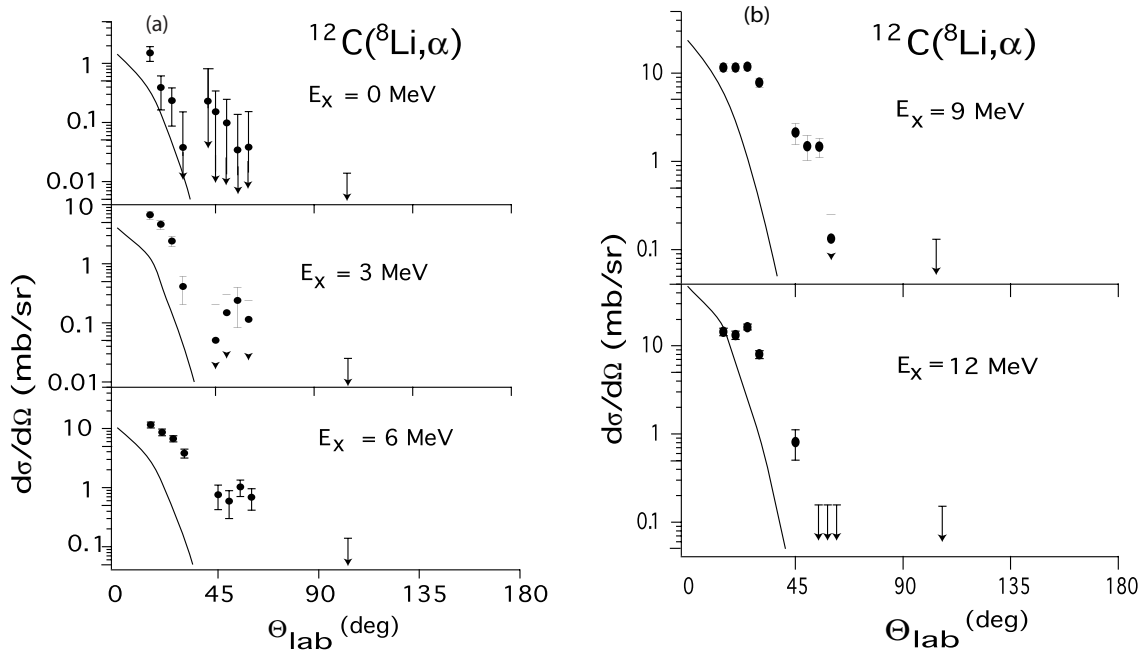


FIG. 4. Angular distributions for $^{nat}\text{C}(^8\text{Li}, \alpha)$ data taken in 3 MeV α -energy bins (labeled in terms of excitation energy in ^{16}N for a direct two-body ^4H transfer reaction). The calculations shown are for a two-source moving-source fragmentation model ($v_R/v_P = 1.0, 0.5,$ and $T_\alpha = 2$ MeV, respectively). The calculations are based on the normalization to the α -energy spectra shown in Fig. 2.

simple projectile breakup, whereas $(v_R/v_P) < 1$ corresponds to partial fusion followed by breakup, or a sequential breakup [12–15]. The projectile momentum at the time of breakup is then added to the internal motion of the α particle, which is assumed to be emitted isotropically in the projectile frame.

A Coulomb-barrier energy cutoff parameter (V_c) typically is also included for charged particles [12]. Often, two or more sources (v_R/v_P and T_α) are needed to fit both the forward-angle and backward-angle data as well as the α -energy spectra.

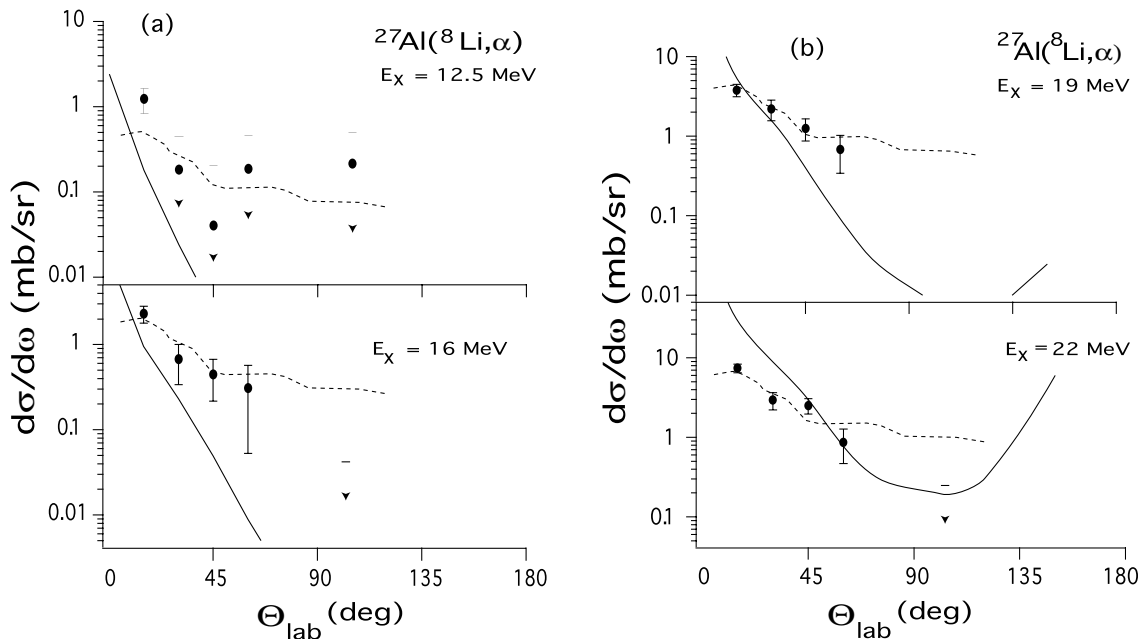


FIG. 5. Same as Fig. 3 but for the ^{27}Al target. A two-source fragmentation model calculation is shown ($v_R/v_P = 1.0, 0.5,$ and $T_\alpha = 2$ MeV, respectively) normalized to the spectra as shown in Fig. 3 (see text). A distorted wave Born approximation (DWBA) calculation (arbitrarily normalized) simulating sequential breakup is also shown (dashed curve; see text).

Fits to the α -energy spectra and angular distributions using this model are shown in several of the figures (Figs. 2 to 5). Two sources can be used to qualitatively describe most of the data for ${}^{27}\text{Al}$: (v_R/v_P) = 1 for forward angles and (v_R/v_P) = 0.5 for back angles, with $T_\alpha = 2$ to 3 MeV (Fig. 5). This is consistent with analyses of similar data taken at higher bombarding energies [e.g., (${}^{16}\text{O}, \alpha$) and (${}^{20}\text{Ne}, \alpha$) at $E/A = 9$ to 85 MeV/nucleon] [12–14]. In particular, the T_α systematics as a function of projectile velocity ($E/\text{nucleon}$) shown in Refs. 12 to 14 would suggest $T_\alpha = 2$ to 3 MeV for ${}^8\text{Li}$ projectiles at ~ 3.5 MeV/nucleon incident beam energy ($E = 27.7$ MeV). Thus, most of the ${}^{27}\text{Al}$ data (Fig. 3) and perhaps some of the ${}^{\text{nat}}\text{C}$ data at low α energies (Figs. 2 and 4) appear to be qualitatively described by the moving-source fragmentation model with a reasonable set of model parameters. In contrast, the spectra and cross sections for ${}^{\text{nat}}\text{C}$ at high α energies [Figs. 2 and 4(a)] are not compatible with this model.

B. Sequential breakup

As noted below for ${}^8\text{Li} + {}^{208}\text{Pb}$, sequential breakup (i.e., inelastic Coulomb or nuclear excitation of ${}^8\text{Li}$ above its breakup threshold) can be a major contributor to projectile breakup. Although this can be incorporated in the moving-source model (see above), an alternate method that is likely to be more appropriate at low bombarding energies is the coupled-channels distorted wave Born approximation (CCDWBA) [15]. The CCDWBA calculations generally produce angular distributions for the heavy fragments (e.g., α particles) similar in shape [e.g., for ${}^6\text{Li} \rightarrow \alpha + d$ (see Sec. IV)] to that expected for projectile excitation (usually via $E1$ excitation). This is not unreasonable if the heavy breakup fragment is emitted in the forward direction with respect to the projectile motion. We can thus qualitatively simulate a CCDWBA sequential breakup angular distribution via a DWBA calculation for $E1$ inelastic projectile excitation (see Sec. IV). Such calculations are shown in Fig. 5 for ${}^8\text{Li} + {}^{27}\text{Al}$, where we assume an $E1$ excitation in ${}^8\text{Li}$ at 6 MeV (i.e., at an energy just above the breakup threshold for ${}^8\text{Li}$). The calculation, which has been arbitrarily normalized but has a magnitude expected for such a process, gives a good representation of the data for ${}^{27}\text{Al}$.

As indicated above, the high energy α spectra (Fig. 2) for ${}^{\text{nat}}\text{C}$ are not consistent with those expected for projectile breakup, so sequential breakup calculations were not performed for ${}^{\text{nat}}\text{C}$. Instead, those data were analyzed with two-body transfer models (direct and sequential), which are consistent with the spectra observed.

C. Direct ${}^4\text{H}$ cluster-transfer calculations

We have performed selective calculations using the finite-range distorted wave Born approximation (FRDWBA) [16] and assuming a direct ${}^4\text{H}$ cluster transfer for ${}^{12}\text{C} \rightarrow {}^{16}\text{N}$. We use various optical-model potentials extrapolated from fits to measured ${}^8\text{Li}$ and α elastic scattering [4,5,17]. The ${}^4\text{H}$

cluster ($J^\pi = 2^-$) is assumed to be bound in the projectile [18] with angular momentum $l = 1\hbar$ at the ${}^4\text{H}$ separation energy [and similarly for various (J^π, E_x) levels [11] in the residual nucleus ${}^{16}\text{N}$]. Owing to the $J^\pi = 2^-$ spin and parity of ${}^4\text{H}$, multiple l transfers are allowed. Combined with the limited angular resolution ($\sim 8^\circ$ FWHM), the calculated angular distributions (Fig. 6) are much less diffractive in shape than the simple calculation shown in Ref. [6]. Nonetheless, there are some notable features seen in the data. Specifically, the data exhibit less forward peaking than expected for projectile breakup, and as noted previously, breakup cannot produce the high energy α particles observed (Fig. 2). Since we are primarily interested in the qualitative features of the FRDWBA calculations (e.g., the overall structure and falloff with angle), we have assumed ${}^4\text{H}$ transfers to high-spin levels in ${}^{16}\text{N}$, ($J^\pi = 2^-$ or 3^-), which should be the major components of the observed cross sections. Again due to the multiple l transfers involved, FRDWBA angular distributions for other final J^π levels will be qualitatively similar. (Although a direct proton transfer reaction can also produce α s, the Q value is not sufficient to produce the high energy α s we observe here).

Perhaps surprisingly [7], the direct-transfer FRDWBA calculations (Fig. 6) resemble the observed angular distributions rather well. The general falloff with angle and the broad diffractionlike features in the data are qualitatively reproduced. This suggests that a two-body cluster-transfer mechanism (apparently corresponding to population of levels at low excitation in ${}^{16}\text{N}$) is likely responsible for the large cross sections observed for ${}^{12}\text{C} ({}^8\text{Li}, \alpha)$.

As a further test of the above hypothesis, we have done calculations using the same ${}^4\text{H}$ transfer model and compared these (see Fig. 7) with the data previously obtained [4] on carbon at $E({}^8\text{Li}) = 14.8$ MeV. The FRDWBA calculations (again owing to the multiple l transfers allowed, along with the finite detector angular acceptance) are not as diffractive as the calculation shown in Ref. [6]. In fact, they more closely reproduce the observations. However, as discussed in Ref. [7], the extraction of the corresponding ${}^4\text{H}$ “spectroscopic factors” may not be very meaningful, as these are very model dependent for projectiles such as ${}^8\text{Li}$ and extended, loosely bound clusters such as ${}^4\text{H}$. In such cases, extraction of reduced widths would be more meaningful. Nonetheless, within a reasonable range of bound-state, nuclear-spin, and optical-model parameters, the data can be reproduced with ${}^4\text{H}$ “spectroscopic factors” near unity for ${}^8\text{Li}$ and ${}^{16}\text{N}$. But as implied in Ref. [7] and as indicated below, a direct two-step sequential transfer can give essentially similar results.

In retrospect, we note that we also have observed [19] very large cross sections for the reaction ${}^8\text{Li} (p, \alpha){}^5\text{He}$. This result is especially of interest in understanding the nucleosynthesis of light elements. These data indicate a large parentage of ${}^8\text{Li}$ as ${}^4\text{H} + {}^4\text{He}$, which would enhance the probability of ${}^8\text{Li} + p \rightarrow {}^4\text{He} + {}^5\text{He}$, as we have observed. This would also favor a direct ${}^{12}\text{C} ({}^8\text{Li}, \alpha)$ reaction, as suggested by the present data for ${}^{\text{nat}}\text{C}$. It also is consistent with the cluster-model calculations by Varga *et al.*, which have been used to describe the properties of the neutron-rich isotopes of Li, including ${}^8\text{Li}$ [18].

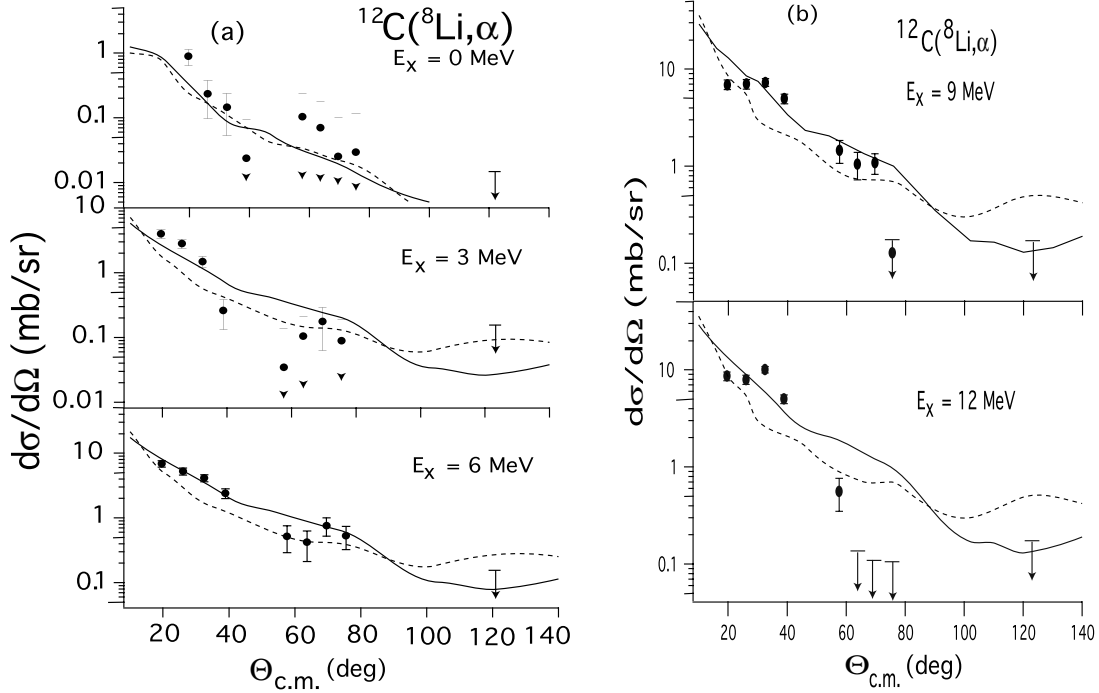


FIG. 6. Angular distributions for $^{nat}\text{C}(^8\text{Li}, \alpha)$ data taken in 3 MeV α -energy bins (labeled in terms of excitation energy in ^{16}N for a direct two-body ^4H transfer reaction). The calculations shown are typical FRDWBA ^4H cluster-transfer calculations arbitrarily normalized to the data shown (solid curve, $J_f^\pi = 3^-$; dashed curve, $J_f^\pi = 2^-$). The calculations have been averaged over angular acceptance of the detector. Scattering angles and cross sections are given in the center of mass (c.m.) system for $^{12}\text{C}(^8\text{Li}, \alpha)^{16}\text{N}$.

Given the apparent direct ^4H transfer observed on ^{nat}C , it would be of interest to look for the analog of ^4H transfer, i.e., ^4Li transfer, and in particular the reaction $^{12}\text{C}(^8\text{B}, \alpha)^{16}\text{F}$ using a secondary ^8B RNB.

D. Multi-step direct transfer

We previously have observed [3,4,8,10] large cross sections for the $(^8\text{Li}, ^7\text{Li})$ one-neutron direct transfer reaction on various targets including ^{12}C . Since this reaction is exothermic, certain transfer-reaction Q values correspond to the optimum ($Q_{\text{opt}} \sim 0$) for a heavy-ion induced neutron transfer. This results in large cross sections even at near-barrier energies [8,10]. Likewise, it is known that ^7Li has a high parentage as $\alpha + t$. Both $(^7\text{Li}, t)$ and $(^7\text{Li}, \alpha)$ direct transfer reactions on targets with $A \approx 12$ have large cross sections (see e.g., the reaction listings in Ref. [20]).

We have performed some simple semiclassical calculations to simulate the angular distributions one might expect from a two-step sequential transfer, e.g., neutron transfer followed by ^3H (i.e., triton) transfer. In a semiclassical model [21], i.e., one modified to include nuclear absorption in the elastic channels, one can relate a given transfer cross section (σ_t) to the elastic scattering cross section $\sigma_{\text{el}}(\theta)$ at a given angle:

$$\sigma_t(\theta) = P_t(\theta) \sigma_{\text{el}}(\theta). \quad (1)$$

Here, $P_t(\theta)$ is the probability function for the transfer process. This assumes that the incoming and outgoing elastic scattering

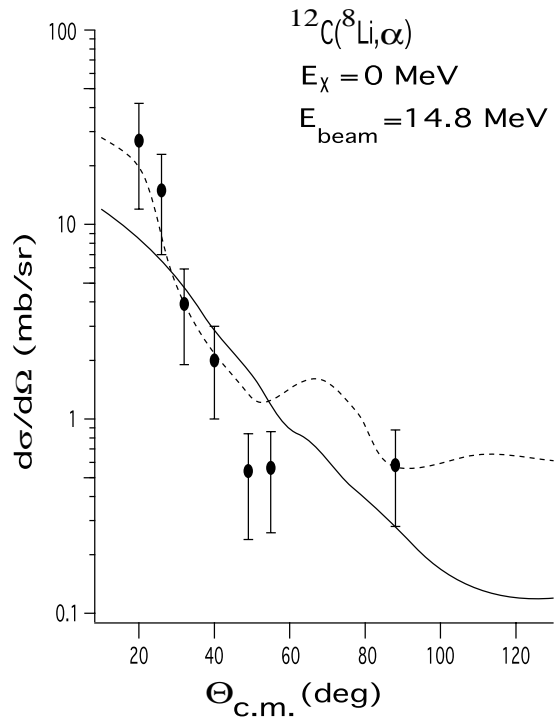


FIG. 7. Same as Fig. 6, but with calculations performed at $E(^8\text{Li}) = 14.8$ MeV and compared with the corresponding $^{12}\text{C}(^8\text{Li}, \alpha)$ data taken from Ref. [4].

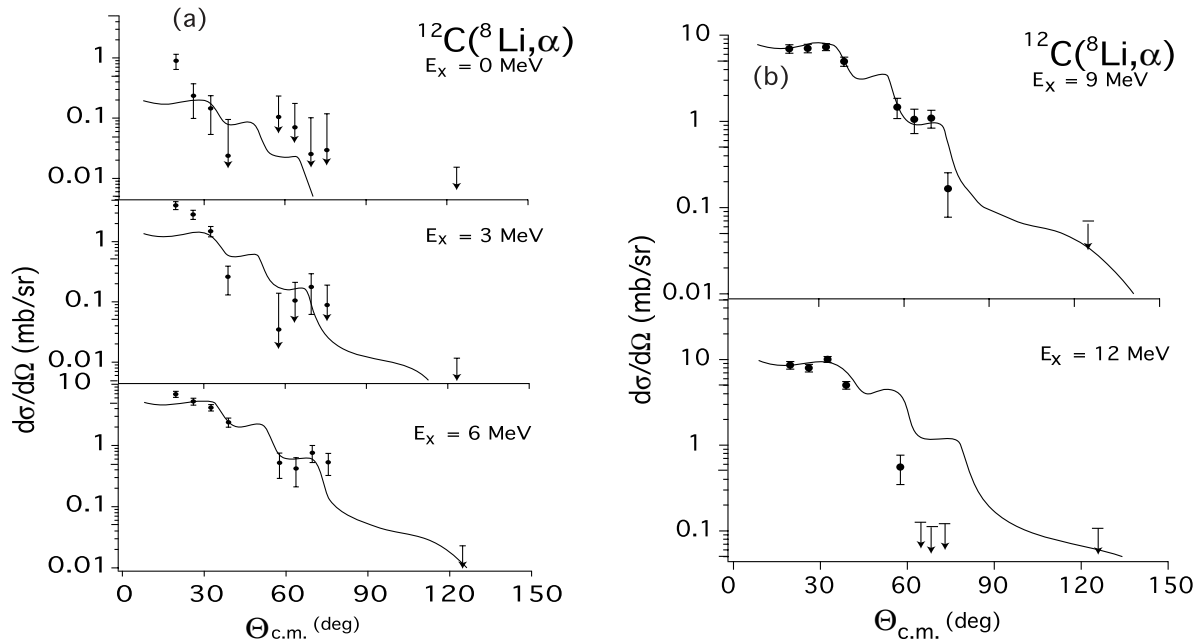


FIG. 8. A semiclassical sequential transfer calculation for $^{12}\text{C}(^8\text{Li}, \alpha)^{16}\text{N}$ compared with a one-step ^4H transfer calculation (arbitrarily normalized) and the experimental data.

channels are similar, as is usually the case for low energy heavy ions. A sequential, two-step transfer $\sigma_{st}(\theta)$ can then be approximated by

$$\sigma_{st}(\theta) = P_{t1}(\theta)P_{t2}(\theta)\bar{\sigma}_{el}(\theta), \quad (2)$$

where $\bar{\sigma}_{el}(\theta)$ is a suitable average [21] of the incident and outgoing elastic scattering.

We can now invoke FRDWBA to calculate $P_{t1}(\theta)$ and $P_{t2}(\theta)$ separately, using calculated values of $\sigma_{el}(\theta)$ which have been fitted to observed data [4] where possible [e.g., $P_{t1}(\theta) = \sigma_{t1}(\theta)/\sigma_{el}(\theta)$]. We have done this for $^{12}\text{C}(^8\text{Li}, \alpha)^{16}\text{N}$ as a $^{12}\text{C}(^8\text{Li}, ^7\text{Li})(^7\text{Li}, \alpha)^{16}\text{N}$ transfer, and the results are shown in

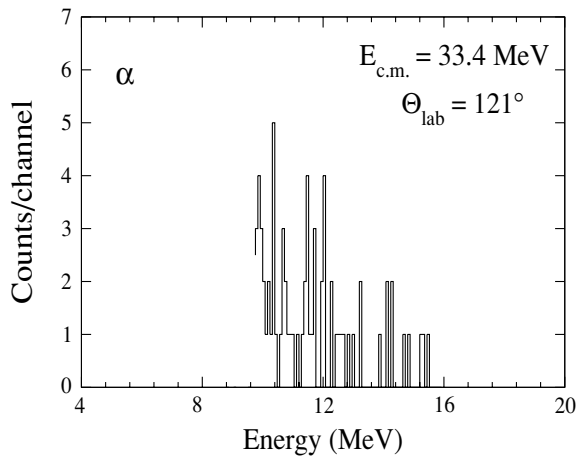


FIG. 9. Energy spectrum of α particles observed from $^8\text{Li} + ^{208}\text{Pb}$ at $E_{c.m.}(^8\text{Li}) = 34.4$ MeV (Ref. [10]; Prof. E. Aguilera, private communication).

Fig. 8, along with the experimental data and direct ^4H transfer calculations.

These calculations are less forward peaked than those for either simple breakup ($v_R/v_P = 1$) or one-step transfer, and

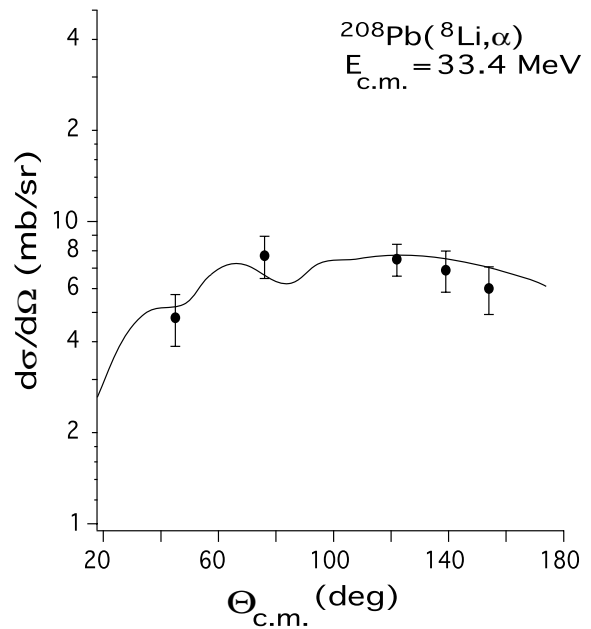


FIG. 10. Angular distribution of α particles from $^8\text{Li} + ^{208}\text{Pb}$ at $E_{c.m.}(^8\text{Li}) = 33.4$ MeV (Ref. [10]) compared with a sequential-breakup calculation extrapolated from those shown in Ref. [23] for $^6\text{Li} + ^{208}\text{Pb}$ at a comparable energy. The latter has been slightly renormalized to fit the present data.

they are also somewhat less diffractive than the latter but otherwise are very similar [22]. Like the one-step cluster-transfer calculations, the angular distributions calculated for multistep transfer are similar to the data observed for $^{12}\text{C} (^8\text{Li}, \alpha) \rightarrow ^{16}\text{N}$ (at low E_x).

IV. $^{208}\text{Pb} (^8\text{Li}, \alpha)$ REACTION

As noted, the bombarding energy used in the present experiment is at or below the Coulomb barrier for ^8Li incident on ^{208}Pb [10]. Still, based on the large cross sections observed for $^{12}\text{C} (^8\text{Li}, \alpha)^{16}\text{N}$ and the large (^8Li , ^7Li) transfer cross sections observed on ^{208}Pb at slightly higher energies, [8, 10, 21], we might have expected measurable ($^8\text{Li}, \alpha$) cross sections for any direct reaction process if, for example, near-barrier neutron “tunneling” were significant. Few if any events attributable to a direct ($^8\text{Li}, \alpha$) mechanism ($Q = 4.9$ MeV) were observed. However, low energy α production cross sections were obtained in a companion experiment [10] done at $E_{\text{c.m.}}(^8\text{Li}) = 34.4$ MeV where time of flight was used to separate reaction α s from the $^4\text{He}^{++}$ contaminant in the secondary ^8Li beam (Fig. 9). This permitted measurements for the α -energy regime corresponding to $^8\text{Li} \rightarrow \alpha + (t + n)$ breakup ($Q \approx -4.5$ MeV), which was obscured by the $^4\text{He}^{++}$ beam contamination in the present experiment (Fig. 1).

The angular distribution obtained [10] for the lower energy “breakup” α s observed at $E(^8\text{Li}) = 34.4$ MeV (Fig. 9) is shown in Fig. 10. The solid curve shown is a sequential breakup model calculation done for $^6\text{Li} + ^{208}\text{Pb}$ at a comparable energy [23]. We expect ^6Li and ^8Li to behave similarly since both have, for example, large Coulomb-excitation cross sections [24, 25]. In fact, the curve shown is only slightly renormalized from the $^6\text{Li} + ^{208}\text{Pb}$ calculation [23]. As with direct one-step breakup, sequential breakup yields a multibody α -energy spectrum with α energies well below those for a direct two-body ($^8\text{Li}, \alpha$) transfer reaction. Sequential fragmentation models have been successful [26–30] in describing similar ($^6\text{Li}, \alpha$) and ($^7\text{Li}, \alpha$) cross sections on heavy targets including ^{208}Pb (in some cases using polarized beams [27]) or via measurement of

coincident α , t , and other fragments [28,29]. (In general, the most complete description requires invoking several closely related breakup mechanisms [26–30]).

The lack of high energy α particles from ^{208}Pb in the present experiment and at $E_{\text{c.m.}}(^8\text{Li}) = 34.4$ MeV, along with the lower energy α s and their angular distributions observed at the latter energy, appears to be compatible with predominantly sequential breakup mechanisms for $^{208}\text{Pb} (^8\text{Li}, \alpha)$ at near-barrier energies.

V. CONCLUSION

We have observed the energy spectra and angular distributions of energetic α particles emitted from the ($^8\text{Li}, \alpha$) reaction on $^{\text{nat}}\text{C}$, ^{27}Al , and ^{208}Pb at $E(^8\text{Li}) = 27.7$ MeV. The data for ^{27}Al appear consistent with simple fragmentation or sequential breakup models. Likewise, the α -energy spectra and upper limits for cross sections on ^{208}Pb obtained in the present experiment, along with data previously measured at a somewhat higher bombarding energy, are suggestive of a sequential breakup mechanism for α production from ^{208}Pb . In contrast, the high energy α data for $^{\text{nat}}\text{C}$ are indicative of a direct ^4H transfer mechanism, as either a one-step cluster transfer or sequential transfer corresponding to population of levels at low excitation in ^{16}N , including those near the ground state. In any case, independent of the exact nature of the transfer mechanism, since RNB-induced “exotic” multinucleon direct transfer reactions can potentially lead to the production of nuclei far from stability and, for example, determination of nuclear properties such as masses (or useful limits on these) far from stability, these reactions warrant further study.

ACKNOWLEDGMENTS

We thank Dr. L. Lamm, Dr. S. Pieper, and Prof. E. Aguilera for their assistance. This work was supported in part by NSF contracts PHY-98-04869, 98-70262, 99-01133, 00-72314, and 02-44989.

-
- [1] W. Liu, Ph.D. thesis, University of Michigan, 1990.
 - [2] J. J. Kolata, F. D. Becchetti, W. Z. Liu, D. A. Roberts, and J. W. Jänecke, *Nucl. Instrum. Methods* **40/41**, 503 (1989).
 - [3] F. D. Becchetti and J. J. Kolata, in *Proceedings of the 14th International Conference on the Application of Accelerators in Research and Industry, Denton, Texas, 1996*, edited by J. L. Duggan and I. L. Morgan, AIP Conf. Proc. No. 392, 369 (AIP Press, Woodbury, NY, 1997).
 - [4] F. D. Becchetti, W. Z. Liu, K. Ashktorab, J. F. Bajema, J. A. Brown, J. W. Jänecke, D. A. Roberts, J. J. Kolata, K. L. Lamkin, A. Morsad, R. J. Smith, X. J. Kong, and R. E. Warner, *Phys. Rev. C* **48**, 308 (1993).
 - [5] R. J. Smith, J. J. Kolata, K. Lamkin, A. Morsad, F. D. Becchetti, J. A. Brown, W. Z. Liu, J. W. Jänecke, D. A. Roberts, and R. E. Warner, *Phys. Rev. C* **43**, 2346 (1991).
 - [6] D. Miljanic, S. Blagus, M. Lattuada, N. Soic, and C. Spitaleri, *Phys. Rev. C* **52**, 1140 (1995).
 - [7] F. D. Becchetti, *Phys. Rev. C* **52**, 1142 (1995).
 - [8] M. Y. Lee, Ph.D. thesis, University of Michigan, 2002.
 - [9] M. Y. Lee *et al.*, *Nucl. Instrum. Methods Res. A* **422**, 536 (1999); F. D. Becchetti, M. Y. Lee, T. W. O'Donnell, D. A. Roberts, J. J. Kolata, L. O. Lamm, G. Rogachev, V. Guimarães, P. A. DeYoung, and S. Vincent, *Nucl. Instrum. Methods Res. A* **505**, 377 (2003).
 - [10] J. J. Kolata *et al.*, *Phys. Rev. C* **65**, 054616 (2002).
 - [11] C. M. Lederer and V. S. Shirley, *Table of Isotopes* (Wiley, New York, 1978).
 - [12] T. C. Awes, S. Saini, G. Poggi, C. K. Gelbke, D. Cha, R. Legrain, and G. D. Westfall, *Phys. Rev. C* **25**, 2361 (1982).

- [13] R. Wada *et al.*, Phys. Rev. C **39**, 497 (1989).
- [14] S. Shaheen, F. D. Becchetti, D. A. Roberts, J. W. Jänecke, R. L. Stern, and A. Nadasen, Phys. Rev. C **42**, 1519 (1990); D. A. Roberts, F. D. Becchetti, J. A. Brown, J. W. Jänecke, D. Shen, Z. W. Yin, and A. Nadasen, *ibid.* **45**, 726 (1992).
- [15] I. J. Thompson, Comput. Phys. Rep. **7**, 167 (1988).
- [16] P. D. Kunz computer code DWUCK5 (unpublished); H. H. Macfarlane and S. Pieper, computer code PTOLEMY, ANL Report ANL-76-11 (unpublished).
- [17] C. M. Perey, and F. G. Perey, At. Data Nucl. Data Tables **17**, 1 (1976).
- [18] K. Varga, Y. Suzuki, and I. Tanihata, Phys. Rev. C **52**, 3013 (1995).
- [19] F. D. Becchetti, J. A. Brown, W. Z. Liu, J. W. Jänecke, D. A. Roberts, J. J. Kolata, R. J. Smith, K. L. Lamkin, A. Morsad, R. E. Warner, R. N. Boyd, and J. D. Kalen, Nucl. Phys. **A550**, 507 (1992).
- [20] F. Ajzenberg-Selove, Nucl. Phys. **A523**, 1 (1991).
- [21] R. A. Broglia and A. Winther, Phys. Rep. C **4**, 153–98 (1972).
- [22] N. Keeley, T. L. Drummer, and E. E. Bartosz, Phys. Rev. C **67**, 044604 (2003).
- [23] G. Signorini, T. Glodariu, Z. H. Liu, M. Mazzocco, M. Ruan, and F. Soramel, Prog. Theor. Phys. **107**, 1 (2002).
- [24] J. A. Brown, F. D. Becchetti, J. W. Jänecke, K. Ashktorab, D. A. Roberts, J. J. Kolata, R. J. Smith, K. Lamkin, and R. E. Warner, Phys. Rev. Lett. **66**, 2452 (1991).
- [25] R. J. Smith, J. J. Kolata, K. Lamkin, A. Morsad, F. D. Becchetti, J. A. Brown, W. Z. Liu, J. W. Jänecke, D. A. Roberts, and R. E. Warner, Phys. Rev. C **43**, 2346 (1991).
- [26] R. Ost, E. Speth, K. O. Pfeiffer, and K. Bethge, Phys. Rev. C **5**, 1835 (1972).
- [27] N. J. Davis *et al.*, Phys. Rev. C **52**, 3201 (1995).
- [28] C. Signorini *et al.*, Phys. Rev. C **67**, 044607 (2003).
- [29] C. Signorini *et al.*, Eur. J. Phys. A **10**, 249 (2001).
- [30] N. Keeley, J. M. Cook, K. W. Kemper, B. T. Roeder, W. D. Weintraub, F. Maréchal, and K. Rusek, Phys. Rev. C **68**, 054601 (2003).